

# CD44 variant-dependent redox status regulation in liver fluke-associated cholangiocarcinoma: A target for cholangiocarcinoma treatment

Malinee Thanee,<sup>1,2</sup> Watcharin Loilome,<sup>1,2</sup> Anchalee Techasen,<sup>2,3</sup> Eiji Sugihara,<sup>4</sup> Shogo Okazaki,<sup>4</sup> Shinya Abe,<sup>5,6</sup> Shiho Ueda,<sup>5</sup> Takashi Masuko,<sup>5</sup> Nisana Namwat,<sup>1,2</sup> Narong Khuntikeo,<sup>2,7</sup> Attapol Titapun,<sup>2,7</sup> Chawalit Pairojkul,<sup>2,8</sup> Hideyuki Saya<sup>4</sup> and Puangrat Yongvanit<sup>1,2</sup>

<sup>1</sup>Department of Biochemistry, Faculty of Medicine, Khon Kaen University, Khon Kaen; <sup>2</sup>Liver Fluke and Cholangiocarcinoma Research Center, Faculty of Medicine, Khon Kaen University, Khon Kaen; <sup>3</sup>Faculty of Associated Medical Sciences, Khon Kaen University, Khon Kaen, Thailand; <sup>4</sup>Division of Gene Regulation, Institute for Advanced Medical Research, School of Medicine, Keio University, Tokyo; <sup>5</sup>Cell Biology Laboratory, Department of Pharmaceutical Sciences, Faculty of Pharmacy, Kindai University, Higashiosaka; <sup>6</sup>Laboratory of Biological Protection, Department of Biological Responses, Institute for Virus Research, Kyoto University, Kyoto, Japan; Departments of <sup>7</sup>Surgery; <sup>8</sup>Pathology, Faculty of Medicine, Khon Kaen University, Khon Kaen, Thailand

## Key words

CD44v, cholangiocarcinoma, opisthorchiasis, redox status, sulfasalazine

## Correspondence

Puangrat Yongvanit, Department of Biochemistry, Faculty of Medicine, Khon Kaen University, Khon Kaen 40002, Thailand.

Tel: +66-4336-3265; Fax: 66-4334-8386;

E-mail: puangrat@kku.ac.th

and

Hideyuki Saya, Division of Gene Regulation, Institute for Advanced Medical Research, School of Medicine, Keio University, Tokyo 160-8582, Japan.

Tel: +81-3-5363-3982; Fax: 81-3-5363-3982;

E-mail: hsaya@a5.keio.jp

## Funding Information

Thailand Research Fund and Khon Kaen University Research Fund; Faculty of Medicine, Khon Kaen University; Office of the Higher Education Commission, Ministry of Education, Culture, Sports, Science and Technology of Japan.

Received March 31, 2016; Revised May 4, 2016; Accepted May 11, 2016

Cancer Sci 107 (2016) 991–1000

doi: 10.1111/cas.12967

CD44 is a single transmembrane protein that is involved in several physiological and pathological processes, including cancer development.<sup>(1,2)</sup> It is expressed in a wide variety of isoforms and can be used as a cell surface marker in order to identify CSCs in many cancer types.<sup>(3–6)</sup> Moreover, expression of CD44v on the cell surface stabilizes xCT and contributes GSH synthesis for ROS defense. xCT is a cystine–glutamate transporter that promotes cystine uptake and then its conversion to cysteine (a rate-limiting step in GSH synthesis).<sup>(7)</sup>

The oxidative stress affects the cellular behavior through intracellular signaling responses such as the MAPK pathways, especially p38<sup>MAPK</sup>. It is involved in cell differentiation, apoptosis, and autophagy through the activation of several kinase proteins; for instance, p21 is an important cell cycle inhibitor,<sup>(8)</sup> resulting in G<sub>1</sub> cell cycle arrest,<sup>(9)</sup> senescence,<sup>(10)</sup> and apoptosis.<sup>(11)</sup> Furthermore, an increase in Atg proteins through

Expression of CD44, especially the variant isoforms (CD44v) of this major cancer stem cell marker, contributes to reactive oxygen species (ROS) defense through stabilizing xCT (a cystine–glutamate transporter) and promoting glutathione synthesis. This enhances cancer development and increases chemotherapy resistance. We investigate the role of CD44v in the regulation of the ROS defense system in cholangiocarcinoma (CCA). Immunohistochemical staining of CD44v and p38<sup>MAPK</sup> (a major ROS target) expression in *Opisthorchis viverrini*-induced hamster CCA tissues (at 60, 90, 120, and 180 days) reveals a decreased phospho-p38<sup>MAPK</sup> signal, whereas the CD44v signal was increased during bile duct transformation. Patients with CCA showed CD44v overexpression and negative-phospho-p38<sup>MAPK</sup> patients a significantly shorter survival rate than the low CD44v signal and positive-phospho-p38<sup>MAPK</sup> patients ( $P = 0.030$ ). Knockdown of CD44 showed that xCT and glutathione levels were decreased, leading to a high level of ROS. We examined xCT-targeted CD44v cancer stem cell therapy using sulfasalazine. Glutathione decreased and ROS increased after the treatment, leading to inhibition of cell proliferation and induction of cell death. Thus, the accumulation of CD44v leads to the suppression of p38<sup>MAPK</sup> in transforming bile duct cells. The redox status regulation of CCA cells depends on the expression of CD44v to contribute the xCT function and is a link to the poor prognosis of patients. Thus, an xCT inhibitor could inhibit cell growth and activate cell death. This suggests that an xCT-targeting drug may improve CCA therapy by sensitization to the available drug (e.g. gemcitabine) by blocking the mechanism of the cell's ROS defensive system.

p38<sup>MAPK</sup> signaling leads to the conversion of LC3-I to LC3-II, resulting in autophagy accumulation and cell death.<sup>(12)</sup>

Cholangiocarcinoma is a malignancy of the bile duct epithelial cells, mainly caused by chronic inflammation due to *Ov* infection in Southeast Asia, especially in northeast Thailand.<sup>(13–16)</sup> Chronic inflammation generates high levels of oxidants, such as ROS and nitrogen species, which can damage cellular biomolecules causing the formation of oxidation products. This can lead to mutations, genetic instability, epigenetic changes, and an alteration of gene expression.<sup>(17,18)</sup> Generally, the damaged cells undergo programmed cell death by apoptosis, autophagy, or necrosis, however, some can survive under high oxidant levels.<sup>(18,19)</sup> How the cell can survive under oxidative stress conditions is still a challenging question that needs to be clarified. The heterogeneity found in solid cancers is supported by a subpopulation of CSCs that is capable of

tumor initiation and self-renewal.<sup>(20)</sup> Redox status regulation in CSCs, which can act as a link between oxidative stress and cancer development, might be one of the mechanisms to explain this phenomenon.

The regulation of redox status in relation to the CD44v-xCT system in CSCs functions not only in driving the damaged cells to enter carcinogenesis processes, but also enables cancer cells to resist anticancer treatment.<sup>(21,22)</sup> Interestingly, an xCT inhibitor (SSZ) has been tested in many studies on the suppression of tumor growth, invasion, and metastasis.<sup>(23–27)</sup> To date, there is no effective, curative chemotherapy for CCA. One explanation for this may be the alteration of the regulation of redox status by the CD44v-xCT system, leading to CCA cell resistance to chemotherapy and linking to the poor prognosis of CCA patients. Hence, the treatment of cancer cells using SSZ, which can inhibit the CD44v-xCT system, may impair the ROS defense mechanism of cancer cells and sensitize them to available anticancer drugs.

In the present study, we report, for the first time, an altered redox status regulating Ov-induced CCA in both a hamster model and humans. We also reveal the function of CD44 in the regulation of the ROS defense system in Ov-induced CCA. Additionally, we examine xCT-targeted CD44v-CSC chemotherapy using SSZ, an xCT inhibitor influencing CCA cell proliferation and survival, possibly through ROS-p38<sup>MAPK</sup>-p21 signaling.

## Materials and Methods

**In vivo animal studies.** *Opisthorchis viverrini* infection with *N*-nitrosodimethylamine in the hamster model has been widely used to study the tumorigenesis processes of bile duct cancer.<sup>(28–30)</sup> The protocol was constructed as previously described.<sup>(29)</sup> In the treatment groups, animals were fed with 50 Ov metacercariae by intragastric intubation combined with the oral administration of 12.5 p.p.m. *N*-nitrosodimethylamine (Sigma-Aldrich, St. Louis, MO, USA) for 30 days; the control group was left untreated. The hamsters were killed at 60, 90, 120, or 180 days. Liver tissues were collected in paraffin blocks or frozen. All experiments were approved by Animal Ethics Committee of Khon Kaen University (Khon Kaen, Thailand) (AEKKU 23/2555).

**Human tissue microarray of CCA samples.** Two human tissue arrays were used in this study. The first was an Ov-associated CCA liver tissue array (97 cases) obtained from the specimen bank of the Liver Fluke and Cholangiocarcinoma Research Center, Faculty of Medicine, Khon Kaen University. The research protocols were approved by the Human Research Ethics Committee, Khon Kaen University (#HE571283) and informed consent was obtained from each subject before surgery. The second was a non-Ov-associated CCA liver tissue array (42 cases) purchased from Abcam (Cambridge, MA, USA).

**Cell culture.** The CCA cell lines, including KKU-214, KKU-213, and KKU-100 were established from CCA patients of Srinagarind Hospital, Khon Kaen University by Professor Banchob Sripa. Certificates of analysis were obtained from Japanese Collection of Research Bioresources Cell Bank, Osaka, Japan. All cell lines were cultured in DMEM (Thermo Fisher Scientific, MA, USA), supplemented with NaHCO<sub>3</sub>, 100 U/mL penicillin, 100 mg/mL streptomycin, and 10% FBS. Cells were maintained in a humidified incubator at 37°C containing 5% CO<sub>2</sub>.

**Antibodies for IHC, immunofluorescence, immunoblot, and flow cytometry analyses.** For IHC and immunofluorescent

staining, anti-CD44s was purchased from BD Bioscience (BD Bioscience, Tokyo, Japan), anti-CD44v8-10 was purchased from Cosmo Bio (Tokyo, Japan), and anti-total and phospho-p38<sup>MAPK</sup> (Tyr180/182) was purchased from Cell Signaling Technology (Danvers, MA, USA.) For immunoblotting, anti-LC3B was purchased from Abcam (Cambridge, UK), anti-p21 was purchased from Santa Cruz (Santa Cruz Biotechnology, CA, USA) and anti-β-actin antibody was purchased from Sigma-Aldrich. For flow cytometry analysis, anti-xCT, which was generated as described previously,<sup>(22)</sup> was kindly donated by the Cell Biology Laboratory and the Biological Protection Laboratory, Kindai University (Higashiosaka, Japan) and Kyoto University (Kyoto, Japan). Anti-CD44v8-10-conjugated FITC and anti-CD44s-conjugated allophycocyanin were purchased from eBioscience (Tokyo, Japan).

**Chemicals.** Three chemicals used in this study, SSZ (an inhibitor of xCT), BSO (a γ-glutamylcysteine synthetase inhibitor), and Trolox (a water-soluble analog of vitamin E that can protect against cell damage by oxidants) were purchased from Sigma-Aldrich.

**Immunohistochemistry analysis.** Liver tissues were fixed in 10% buffered formaldehyde, embedded in paraffin blocks and then sectioned at a thickness of 4 μm. Sections were deparaffinized in xylene and rehydrated in an ethanol series. Immunohistochemical staining was carried out for CD44s, CD44v8–10, and phospho-p38<sup>MAPK</sup> according to standard methods as previously described.<sup>(31)</sup> The sections were observed under a light microscope at ×200 and ×400 magnification (Axioscope A1; Carl Zeiss, Jena, Germany). The scoring system of IHC was previously described.<sup>(32,33)</sup>

**Immunofluorescence analysis.** The tissue sections were processed for IHC staining and retrieved by heating in 0.01 M sodium citrate containing 0.05% Tween-20 (pH 6.0) for 10 min at 110°C. For cell culture, CCA cells were fixed with 4% paraformaldehyde. The samples were then exposed to 3% BSA before being incubated at 4°C overnight with primary antibodies (CD44v8–10, phospho-p38<sup>MAPK</sup>, and p21). The samples were washed three times with TBS, then incubated with Alexa Fluor 647- or 488-conjugated secondary antibodies (Invitrogen, Tokyo, Japan), and mounted in Vestashield mounting medium containing DAPI (Vector Laboratories, Burlingame, CA, USA). Next, the stained tissues were observed under a FV1000-D confocal microscope (Olympus, Tokyo, Japan) at ×200 and ×400 magnification.

**Immunoblot analysis.** The CCA cell lines (1 × 10<sup>5</sup> cells per well) were seeded into 6-well plates for 24 h and then treated with 300 μM SSZ (Sigma-Aldrich). The method was previously described.<sup>(34)</sup> Briefly, equal amounts of protein (15 μg) were treated with SDS sample buffer. The samples were separated on 10% polyacrylamide gels by electrophoresis and transferred onto PVDF membranes. The membranes were incubated with primary antibody against total-p38<sup>MAPK</sup>, phospho-p38<sup>MAPK</sup>, LC3B, and β-actin overnight at 4°C. The proteins were analyzed using chemoluminescence enhancing with an ECL Prime Western Blotting Detection System (GE Healthcare, Little Chalfont, UK). β-Actin expression was used as an internal control.

**Flow cytometry analysis.** For flow cytometry (FACS) analysis, single-cell suspensions were incubated with antibodies to CD44s, CD44v8–10, and xCT for 15 min at 4°C. Apoptotic cells were excluded during flow cytometry by elimination of cells staining positive with propidium iodide (Sigma-Aldrich). Flow cytometry analysis was undertaken with an Attune Acoustic Focusing Cytometer (Life Technologies/Applied Biosystems, Tokyo, Japan).

**CD44 siRNA transfection.** Highly CD44v8–10-expressing CCA cell lines KKU-213 and KKU-214 were used. The CCA cells ( $1 \times 10^5$  cells) were seeded into 6-well plates for 24 h before transfection. Cells were then transfected with either control or specific target siRNAs for 24–96 h using Lipofectamine RNAi MAX reagent (Invitrogen). The siRNA specific to human CD44 mRNA (target 1, 5'-AAAUGGUCGUACAGCAUCTT-3'; target 2, 5'-GUAUGACACAUUAUGCUUCTT-3') was obtained from JbioS (Saitama, Japan). Next, the level of CD44v8–10, xCT, ROS, phospho-p38<sup>MAPK</sup>, and GSH were analyzed after transfection.

**Measurement of GSH content.** The intracellular GSH levels were examined using a GSH-Glo Glutathione Assay kit (Promega, Madison, WI, USA). The samples were harvested and diluted in PBS to  $5 \times 10^3$  cells per well in 96-well black plates. Then GSH-Glo Reaction Buffer containing luciferin-NT and GST was added to the plate and incubated for 30 min. Reconstituted luciferin was then added to the plate and incubated for 15 min. The plate was read in a luminometer. This assay was normalized using a GSH standard solution provided with the kit. Data were expressed as mean  $\pm$  SD of reduced intracellular GSH concentration.

**Measurement of ROS level.** The intracellular ROS levels were determined using DCF fluorescence staining (C6827; Invitrogen). The samples were incubated with 10  $\mu$ M dichloro-dihydro-fluorescein diacetate (DCFH-DA) for 15 min at 37°C, and then twice washed with PBS. The median intensity of DCF fluorescence in 10 000 cells was determined using flow cytometry. The results were analyzed using FlowJo software (Tree Star, San Carlos, CA, USA) and presented as relative fluorescence intensity.

**Cell proliferation and cell cytotoxicity.** The number of viable cells was evaluated with a Cell Titer-Glo luminescence cell viability kit (Promega). Briefly, CCA cells ( $2 \times 10^3$  cells per well) were plated into 96-well black plates for 24 h. Cells were then treated with SSZ (0, 200, 400, 600, 800, or 1000  $\mu$ M) for 24, 48, 72, or 96 h. The luminescence signal was detected on a SpectraMax L microplate reader (Molecular Devices, CA, USA). The experiments were done in triplicate.

**Statistical analysis.** Statistical comparisons were carried out using spss software version 17.0 (IBM, Armonk, NY, USA). The association between protein expression in CCA tissue and patient clinical data was analyzed using the  $\chi^2$ -test. Patient survival was calculated according to Kaplan–Meier with a log-rank test. All analyses were two-tailed and *P*-values < 0.05 were considered statistically significant.

## Results

**CD44 expression during CCA genesis in hamster model.** Immunohistochemical analysis revealed an increasing positive signal of CD44s along with CD44v8–10 in the cytoplasm of the transformed cholangiocytes, including the hyperplastic bile duct, at days 60 and 90, in the dysplastic bile duct at day 120, and the malignant bile duct at day 180. The strongest expression of CD44s and CD44v appeared to occur at days 120 and 180 in both dysplasia and the malignant bile duct epithelia (Fig. 1a). The highest phospho-p38<sup>MAPK</sup> signal (a main target of ROS signaling) was seen in the nucleus of the hyperplastic bile duct cells at day 60. Thereafter, a decreasing level of p38<sup>MAPK</sup> was seen along with the progression of bile duct cell transformation (Fig. 1a). Moreover, with a high CD44v8–10 expression of the bile duct cells there was a negative signal of p38<sup>MAPK</sup> activation; conversely, positive p38<sup>MAPK</sup> activation

was seen in low CD44v8–10 expressed bile duct cells during cholangiocarcinogenesis (Fig. 1b). These results indicate that CD44s and CD44v8–10 are highly expressed during cholangiocarcinogenesis and are related to the increased regulation of redox status. This provides an advantage for cancer cells to survive in the high oxidative stress conditions that are associated with the CD44v8–10–xCT system. The resistant cells may increase and develop into tumor cells.

**CD44 expression in CCA patients.** Chronic inflammatory responses of cytokine signaling are the key molecular mechanisms underlying Ov-associated CCA, whereas aberrant growth factor signaling plays a major role in non-Ov associated CCA.<sup>(35)</sup> We thus evaluated the different patterns of CD44v8–10 and p38<sup>MAPK</sup> expression in Ov- and non-Ov-related CCA liver tissues. Our results showed that there was a negative association between phospho-p38<sup>MAPK</sup> and CD44v8–10 in Ov-associated CCA patients (76%). This was higher than in non-Ov-associated CCA patients (52%), although CD44v8–10<sup>high</sup> expression was seen in non-Ov-related CCA patients (50%), which was as high as in Ov-related CCA patients (43%; Fig. 2a). A negative correlation between CD44v8–10 and phospho-p38<sup>MAPK</sup> expression in Ov-associated CCA patients was observed ( $-0.098$ ,  $P = 0.171$ ), whereas a positive correlation of CD44v8–10 with phospho-p38<sup>MAPK</sup> was seen in non-Ov-associated CCA patients ( $0.121$ ,  $P = 0.137$ ). This finding indicates that the expression of CD44v8–10 in CCA with Ov infection is related with ROS signaling (p38<sup>MAPK</sup>), but it is not seen in patients with non-Ov-associated CCA.

Interestingly, a high membranous CD44v8–10 signal (CD44v8–10<sup>high</sup>) and positive phospho-p38<sup>MAPK</sup> expression was cumulative in 43% (42/97) and 29% (22/97) of CCA cases, respectively (Fig. 2b; Table 1). In addition, the colocalization of CD44v8–10 and phospho-p38<sup>MAPK</sup> showed a CD44v8–10-positive signal that was inversely correlated with p38<sup>MAPK</sup> (Fig. 2c). The CD44v8–10<sup>high</sup> patients with a negative phospho-p38<sup>MAPK</sup> had a significantly shorter survival than CD44v8–10<sup>low</sup> patients with a positive phospho-p38<sup>MAPK</sup> ( $P = 0.030$ ; Fig. 2d). Moreover, CD44s<sup>high</sup> expression was significantly associated with a high level of metastasis ( $P = 0.043$ ) (Table 1). Our observations suggest that CD44v8–10 plays a role in the regulation of the ROS defense system (high CD44v8–10, negative p38<sup>MAPK</sup>), which is linked to a poor prognosis in CCA patients.

**CD44 variants 8–10 regulate cell surface expression of xCT to promote ROS defense in CD44v8–10-positive CCA cell lines.** Based on the expression profile of Ov-induced hamster and human CCA tissues, we next explored the function of CD44v8–10 in relation to the ROS defense system through stabilizing xCT. The levels of CD44s, CD44v8–10, and xCT in three human CCA cell lines (KKU-213, KKU-214, and KKU-100) were evaluated by using flow cytometry analysis. High CD44v8–10 and xCT expression on cell surfaces was found in KKU-213 and KKU-214. For KKU-100, a low signal for both xCT and CD44v8–10 was observed (Fig. 3a). CD44v8–10<sup>high</sup>-KKU-213 and KKU-214 cells were transiently transfected either with two siRNAs of specifically targeted CD44 mRNA (CD44 siRNA) or a control siRNA. The expression of CD44v8–10 was successfully decreased approximately 3-fold compared to the KKU-214 control, whereas a 1-fold suppression was observed in KKU-213. Furthermore, CD44 siRNA-transfected cells had a lower xCT signal than control siRNA-transfected cells (Fig. 3b). These results suggest that CD44v8–10 could stabilize xCT on membranes in CCA cell lines. Thus, we next examined the effects of CD44v8–10 suppression on the regulation of the

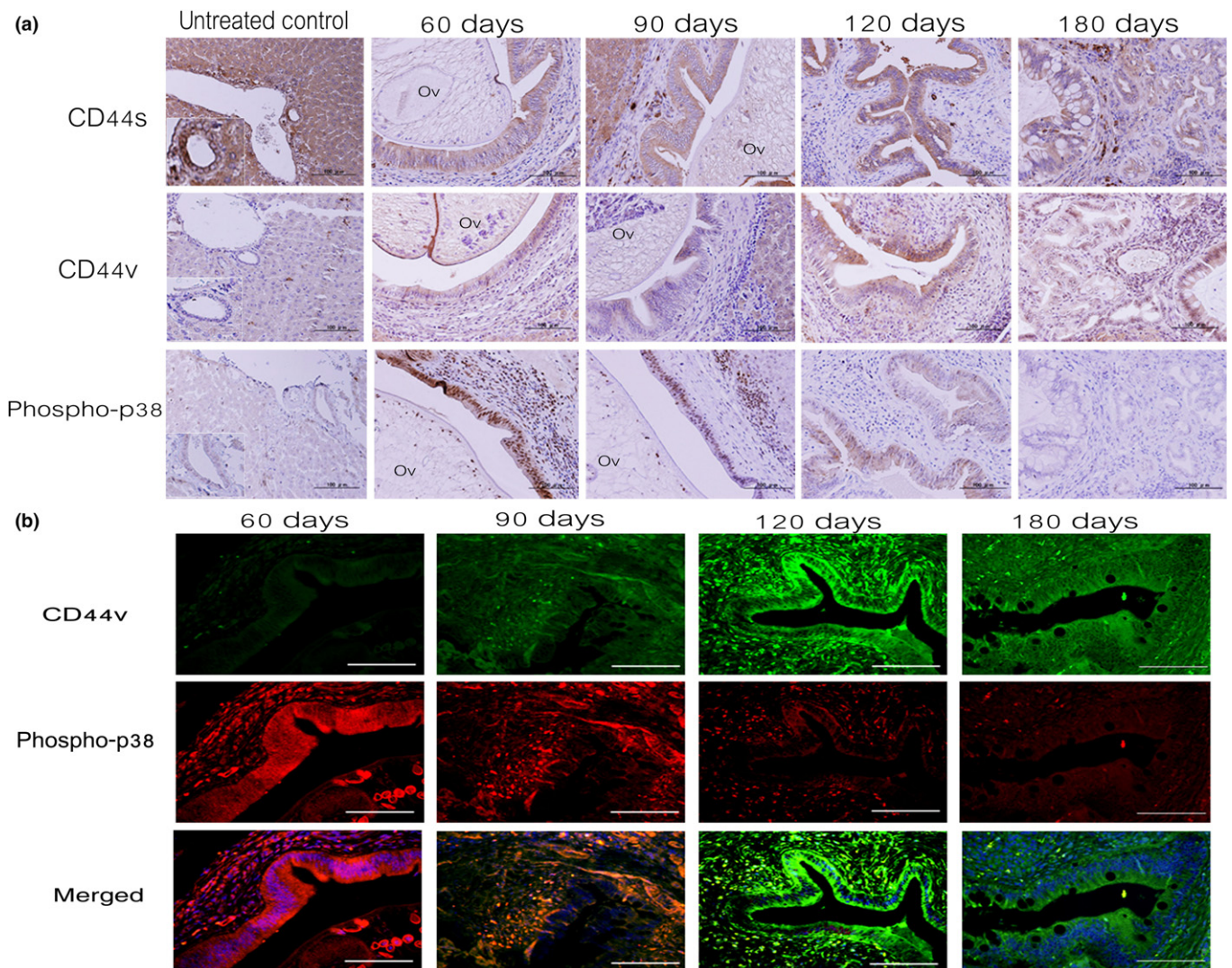


**Fig. 1.** Upregulation of CD44 was negatively associated with downregulation of p38<sup>MAPK</sup> during *Opisthorchis viverrini* (Ov)-induced carcinogenesis in hamster. (a) Increased expression of standard CD44 (CD44s) and CD44 variant (CD44v) and decreased signal of phospho-p38<sup>MAPK</sup> during Ov-induced cholangiocarcinoma genesis at 60, 90, 120, and 180 days post-Ov infection were observed using immunohistochemical techniques. (b) Colocalization shows the converse correlation of CD44v8–10 and phospho-p38<sup>MAPK</sup>. Magnification,  $\times 40$ .

ROS defense system by monitoring GSH and ROS levels either in normal or oxidative stress conditions. The GSH level was clearly decreased whereas the ROS was increased with CD44v8–10 reduction under oxidative stress (Fig. 3c,d). An activation of p38<sup>MAPK</sup>, which regulates several protein kinases involved in cellular function, was seen (Fig. 3e). These results revealed that suppression of the CD44v8–10-xCT system could contribute to the induction of an intracellular ROS level through decreasing GSH synthesis.

**Sulfasalazine suppresses CCA cell proliferation and activation of p38<sup>MAPK</sup>, resulting in induction of autophagic cell death in CCA cell lines.** We next confirmed whether the function of the CD44v8–10-xCT system was related to the regulation of ROS defense by using SSZ. Our observations showed that SSZ-treated CD44v8–10<sup>high</sup>-expressing CCA cells had higher ROS levels than SSZ-treated CD44v8–10<sup>low</sup>-expressing CCA cells. We used BSO, an inhibitor of GSH synthesis, as a positive control. Surprisingly, SSZ-treated CCA cells have intracellular ROS levels as high as BSO-treated cells in high expression

xCT cells (KKU-213 and KKU-214), whereas low expression xCT cells (KKU-100), which were treated with SSZ, had lower ROS levels than BSO-treated cells (Fig. 4a). Similarly, a reduced intracellular GSH level was found after SSZ treatment in parallel with BSO treatment (Fig. 4b). These results suggest that a CD44v8–10-xCT-dependent ROS defense system exists with high CD44v8–10 and xCT expression, whereas low expression cells were not affected. We further examined whether the CD44v8–10-xCT system can be a potential target for CCA treatment. The results clearly showed that KKU-213 and KKU-214 were more sensitive to SSZ treatment than KKU-100 (Fig. 4c). Cell death induction was also inhibited by Trolox treatment, indicating the reverse effect of the oxidative stress phenotype by SSZ treatment (Fig. 4d). Our results show that SSZ-treated cells proliferated significantly more slowly than control cells in all cell lines (Fig. 4e). We also showed that phospho-p38<sup>MAPK</sup>, p21 (cell cycle inhibitor), and LC3B-II (autophagic protein) expression was upregulated after SSZ treatment (Fig. 4f,g), hence an inhibition of cell proliferation

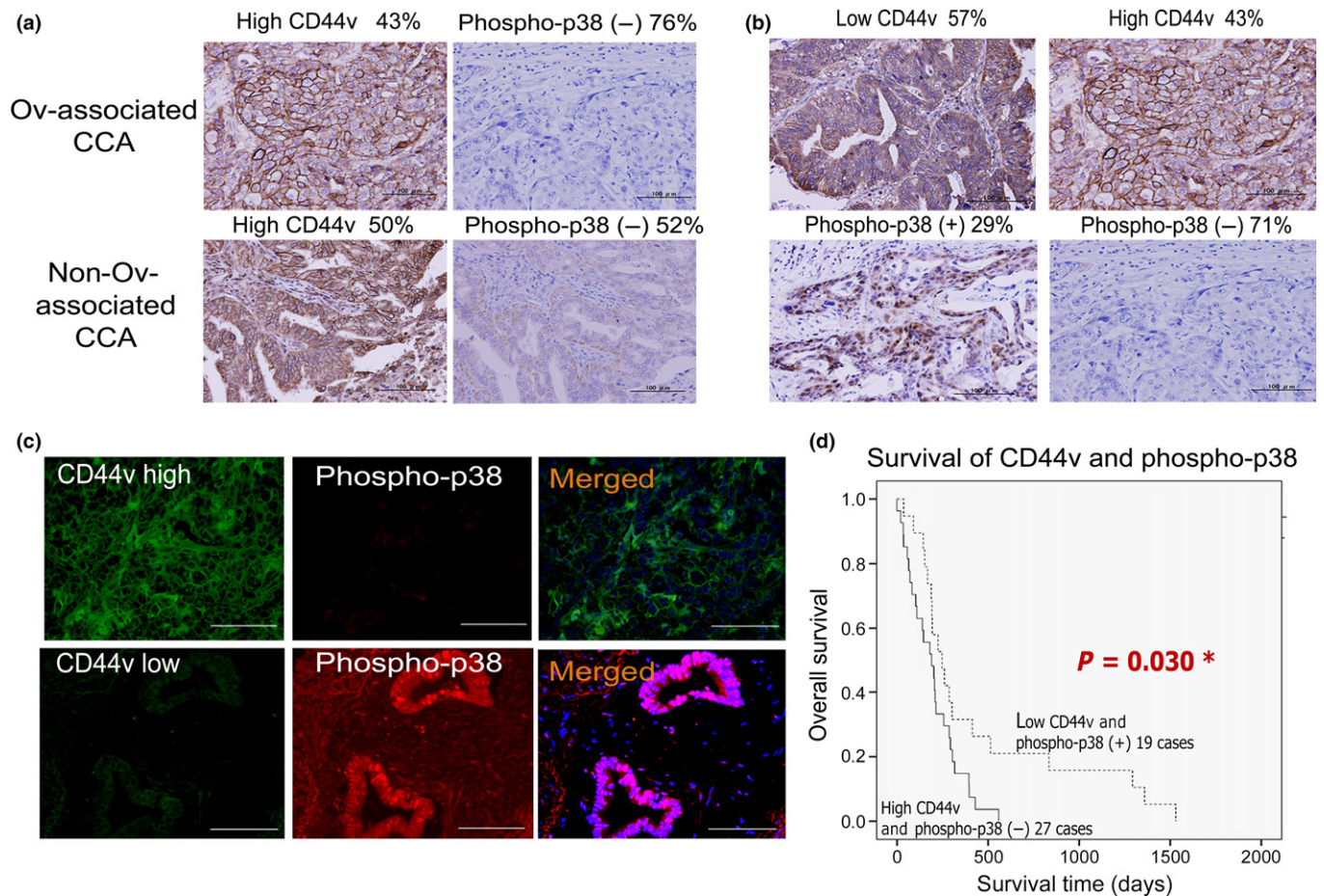


**Fig. 2.** Combination of CD44 variants 8–10 (CD44v8–10) and phospho-p38<sup>MAPK</sup> expression predicts cholangiocarcinoma (CCA) survival. (a) Different expression patterns of CD44v8–10 and phospho-p38<sup>MAPK</sup> in cancer cells of patients with *Opisthorchis viverrini* (Ov)-associated and non-Ov-associated CCA showed that 76% of Ov-associated CCA patients have a negative association between CD44v8–10 and phospho-p38<sup>MAPK</sup> expression. (b) Immunohistochemistry analysis revealed that 43% of CCA patients had high expression of CD44v8–10 and 29% of CCA patients have positive phospho-p38<sup>MAPK</sup> in Ov-associated CCA. (c) Colocalization of Ov-associated CCA tissues indicates that CD44v8–10 expression is conversely related to the phospho-p38<sup>MAPK</sup> signal. (d) Kaplan–Meier method of survival analysis in Ov-associated CCA patients in two groups show CD44v8–10<sup>high</sup> and negative to phospho-p38<sup>MAPK</sup> compared with CD44v8–10<sup>low</sup> and positive to phospho-p38<sup>MAPK</sup>. \* $P < 0.05$  was considered statistically significant.

**Table 1.** Correlation between the expression of standard CD44-positive, CD44 variants 8–10-positive, total p38<sup>MAPK</sup>-positive, and phospho-p38<sup>MAPK</sup>-positive cholangiocarcinoma cells in patients with *Opisthorchis viverrini*-associated cholangiocarcinoma

Clinicopathologic data	n	Expression of CD44						Expression of p38 <sup>MAPK</sup>					
		Standard		P-value	Variant		P-value	Total form		P-value	Active form		P-value
		Low	High		Low	High		Negative	Positive		Negative	Positive	
Age, years													
<58	49	25	24	0.418	31	18	0.222	25	24	0.686	37	12	0.809
≥58	48	20	28		24	24		22	26		38	10	
Sex													
Male	69	30	39	0.380	37	32	0.374	37	32	0.123	52	17	0.596
Female	28	15	13		18	10		10	18		23	5	
Histological types													
Non-papillary	68	28	40	0.126	36	32	0.273	33	35	1.000	54	14	0.442
Papillary	29	17	12		19	10		14	15		21	8	
Metastasis													
No metastasis	45	26	19	0.043*	27	18	0.681	24	21	0.419	35	10	1.000
Metastasis	52	19	33		28	24		23	29		40	12	

\* $P \leq 0.05$  was considered statistically significant.

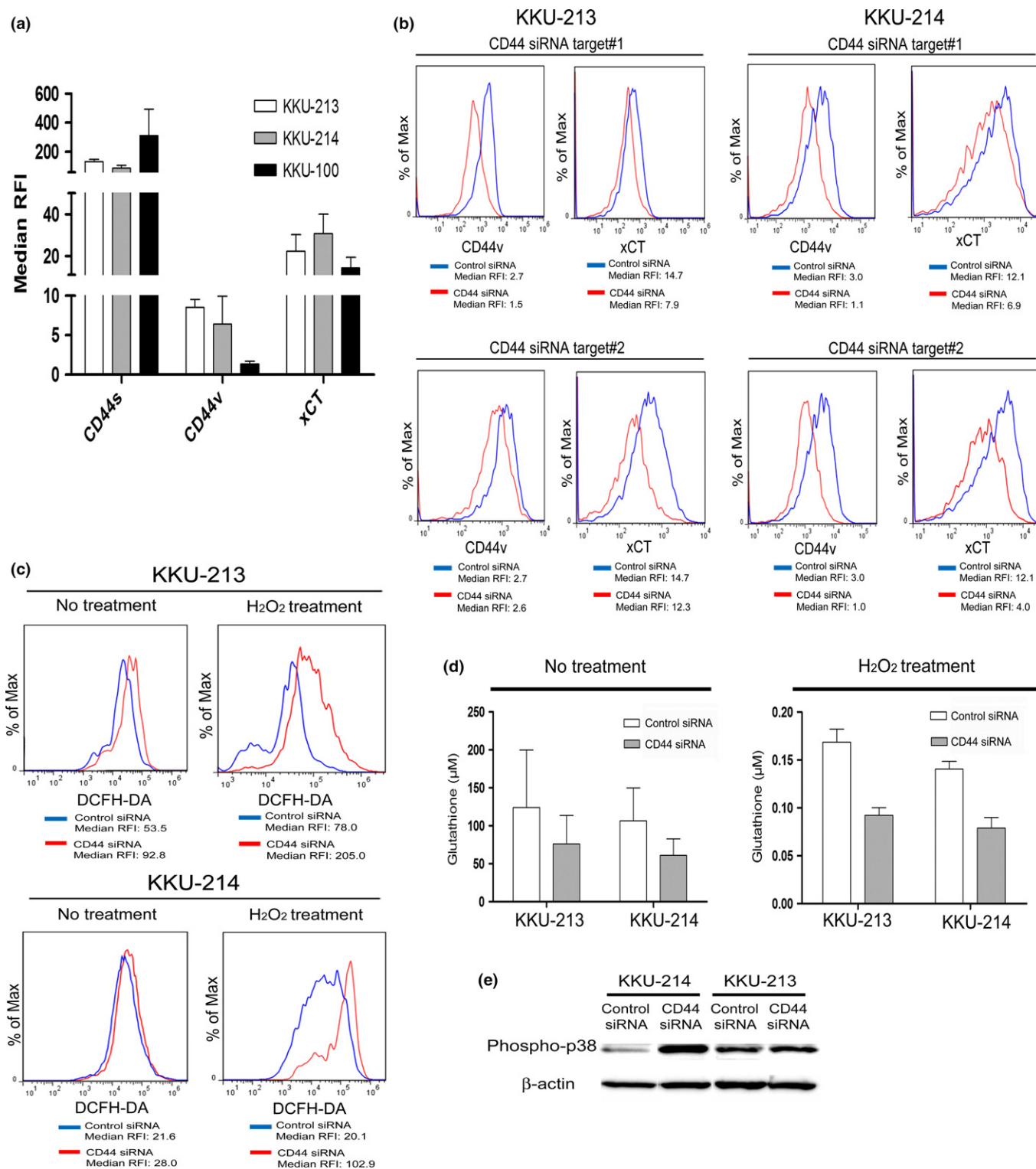


**Fig. 3.** Knockdown of CD44 shows that CD44 variants 8–10 (CD44v8–10) and xCT expression on the surface of cholangiocarcinoma (CCA) cells is related to the regulation of redox status. (a) Basal levels of standard CD44 (CD44s), CD44v8–10 and xCT in CCA cell lines were determined using flow cytometry. (b) Flow cytometric analysis of CD44v8–10 and xCT expression on the cell surface showed that the xCT level was decreased in CCA cells transfected with CD44 siRNAs. Cells with control or CD44 siRNAs transfection were incubated in the presence or absence of 500 μM H<sub>2</sub>O<sub>2</sub> for 20 min, and then stained with dichloro-dihydro-fluorescein diacetate (DCFH-DA) for flow cytometry analysis (c) and glutathione assay (d). (e) Upregulation of phospho-p38<sup>MAPK</sup> was evaluated by Western blotting in knockdown of CD44. RFI, relative fluorescence intensity.

was stimulated by p38<sup>MAPK</sup>, possibly through p21 signaling, and cell death processes were induced by the autophagic pathway. Our findings suggest that SSZ could suppress cell growth

possibly through ROS–p38<sup>MAPK</sup>–p21 signaling and induce cell death through the activation of ROS–p38<sup>MAPK</sup> signaling-dependent autophagic processes.

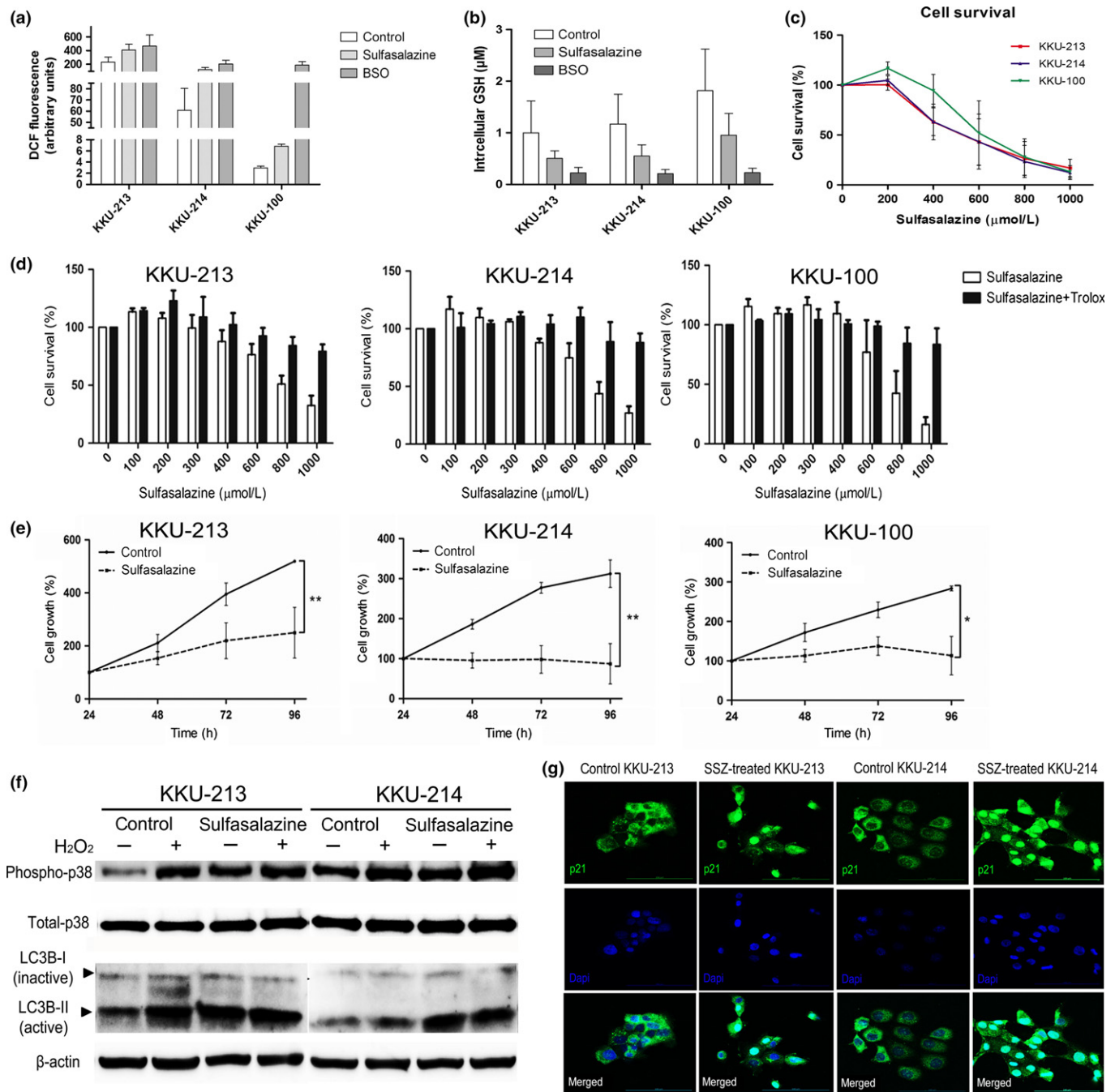


**Fig. 4.** Sulfasalazine (SSZ), an xCT inhibitor, could inhibit cell growth and activate cell death possibly through the reactive oxygen species (ROS)-p38<sup>MAPK</sup>-p21-dependent autophagy pathway. SSZ-treated cholangiocarcinoma (CCA) cell lines showed that the ROS level was increased (a) and reduced glutathione (GSH) was decreased (b). (c) Percentage of CCA cell survival after treatment with various concentrations of SSZ for 48 h, together with the presence or absence of 6-hydroxy-2,5,7,8-tetramethylchroman-2-carboxylic acid (Trolox; antioxidant) (d), showed that CCA cells sensitized to SSZ treatment could recover from antioxidants. (e) Cell proliferation inhibition effect of SSZ on CCA cell lines. \**P* < 0.05; \*\**P* < 0.01. (f) Overexpression of ROS-p38<sup>MAPK</sup> signaling downstream proteins (p38<sup>MAPK</sup>), as well as autophagic-activated proteins (LC3B), was observed. (g) Nuclear localization of p21 (cell cycle inhibitor) was revealed using immunofluorescence. BSO, buthionine sulphoximine.

## Discussion

In the present study, we found an increasing expression of both CD44s and CD44v8–10 starting at day 60 until day 180 after Ov infection along with the transformation of normal bile duct cells to cells with hyperplasia, and dysplasia to CCA, although cytoplasmic CD44 was seen in hamster CCA tissues rather than membrane-positive staining. We hypothesized that

CD44 could move from the membranes of the bile duct cells to localize in the cytoplasm when these cells became malignant.<sup>(36)</sup> Our results indicate that an upregulation of CD44, including CD44s and CD44v8–10, was inversely correlated with downstream ROS signaling phospho-p38<sup>MAPK</sup> expression in the hamster carcinogenesis group when compared to the untreated group. We assumed that an overproduction of

oxidants occurs during Ov-induced cholangiocarcinogenesis. This not only damages biomolecules, but also induces the expression of CD44 as well as CD44 variant forms. Even though oxidant-damaged cells normally undergo programmed cell death, some of the damaged cells, which we believe are those that express CD44, can survive, proliferate, and subsequently transform into tumor cells that eventually develop into tumor mass. A previous study showed that CD44-positive cells in normal mice are supposed to be candidates for the cell origin of gastric CSCs.<sup>(37)</sup> In this study, we hypothesized that CD44-positive cells are also potential candidates for the cell origin of CCA stem-like cells. These cells could be able to adapt their redox status regulation to maintain redox homeostasis during CCA genesis, possibly through enhancing GSH production by way of the CD44v8–10–xCT system, resulting in evasion of cell death. This study provides the first evidence in CCA to explain the linkage between the mechanism of oxidative stress and cancer development through the expression of the CD44 CSC marker, which leads to the alteration of redox regulating status causing cells to resist apoptosis and finally develop into cancer.

Standard CD44 has been reported to contribute to the epithelial–mesenchymal transition process that plays important roles in cancer metastasis through activation of transforming growth factor- $\beta$  and Akt.<sup>(2)</sup> Previous evidence suggests that CCA patients with a high expression of CD44s have a poor prognosis,<sup>(38)</sup> and an *in vitro* study of the reduction of CD44s showed that CD44s expression could facilitate cell invasion and cell migration in CCA.<sup>(39)</sup> Similarly, the present work shows that CD44s<sup>high</sup> expression in CCA patients had significantly higher metastasis potential than CD44s<sup>low</sup> expression. Furthermore, CD44v8–10 enhances mechanisms of the ROS defense system.<sup>(22)</sup> The IHC staining of human CCA tissues indicated the expression of phospho-p38<sup>MAPK</sup> downstream of ROS signaling, which was negatively associated with upregulation of CD44v8–10. We thereby hypothesized that CD44v8–10 might regulate the ROS defense system (high CD44v8–10, negative p38<sup>MAPK</sup>), linking to the poor prognosis for CCA patients.

A relationship between CD44v8–10 and redox status regulation in human CCA tissues was confirmed using an siRNA assay. Our findings revealed that CD44v8–10 regulates redox status by stabilizing xCT, resulting in a reduced GSH level and decrease in the ROS level. This, in turn, led to suppression of p38<sup>MAPK</sup> activation. Furthermore, the cells treated with SSZ also showed the ability to modify their intracellular redox status and suppress the ROS defense system by blocking GSH synthesis. The alteration of redox status can activate ROS–p38<sup>MAPK</sup> signaling, resulting in inhibition of cell growth through the accumulation of p21. Additionally, ROS–p38<sup>MAPK</sup> signaling<sup>(8)</sup> may affect the induction of autophagy through increasing the level of Atg proteins, such as beclin 1 and Atg5.<sup>(12,40–42)</sup>

Many studies have shown that tumor progression, relapse, and metastasis are driven by CSCs, which are identified by cell surface markers including CD44. Recently, it was shown that CD44v8–10, but not CD44s, play roles in the regulation of redox status through specifically interacting with xCT in CSCs. An xCT–plasma membrane amino acid transporter controls the exchange of extracellular cystine and intracellular glutamate (xc<sup>-</sup> system), which contributes to GSH synthesis. This covalently interacts with CD98hc.<sup>(43)</sup> Moreover, several studies have shown that high xCT expression is associated with cell proliferation and anticancer drug-resistant properties.<sup>(44)</sup> Additionally, treatment of the xCT inhibitor selectively induced

apoptosis in CD44v8–10-expressing cells without affecting CD44v8–10-negative cells in head and neck squamous cell carcinoma.<sup>(27)</sup>

Imbalance of oxidants/antioxidants leads to the alteration of cell signaling, especially the ROS–p38<sup>MAPK</sup> signal. p38<sup>MAPK</sup> is a class of MAPK that negatively controls carcinogenesis. p38<sup>MAPK</sup> responds to stress stimuli, and is involved in cell differentiation, apoptosis, and autophagy. Moreover, p38<sup>MAPK</sup> has been reported to contribute to suppression of carcinoma development by inhibiting cell growth and the induction of cell death. It can directly activate p21, which is an important cell cycle inhibitor,<sup>(8)</sup> resulting in G<sub>1</sub> cell cycle arrest<sup>(9)</sup> and senescence.<sup>(10)</sup> Furthermore, it has also been reported that p38<sup>MAPK</sup> signaling could trigger autophagy to conversion of LC3B-I to LC3B-II through increasing the level of Atg proteins.<sup>(12)</sup> Therefore, the inhibition of the CD44v8–10–xCT system contributes an oxidative stress to cancer cells, which enhances intracellular ROS levels, resulting in suppression of p38<sup>MAPK</sup>- and p21-mediated proliferation inhibition as well as stimulation of p38<sup>MAPK</sup>-mediated autophagic pathway in CCA.

Although Ov infection is defined as a major risk factor of CCA in Thailand, there are also several other causes of CCA development. This study shows a distinct pattern of regulating redox status protein in Ov-associated and non-Ov-associated CCA. We observed that the negative association of CD44v8–10 and p38<sup>MAPK</sup> expression in Ov-associated CCA patients correlated with clinicopathological data, whereas this was not seen in non-Ov-associated CCA patients. We previously reported that Ov-induced CCA can cause DNA damage through oxidant production.<sup>(30,45,46)</sup> Therefore, Ov infection may lead to increased expression of CD44, which might, in turn, interact with xCT and enhance antioxidants to maintain the intracellular redox status by taking up cystine, the key factor in GSH synthesis. Our previous study also showed differences in the frequency of gene mutation between Ov and non-Ov associated CCA: *p53* mutation was frequently found in Ov-associated CCA, whereas *KRAS* mutation was frequently observed in non-Ov CCA.<sup>(47)</sup> Activity of p53 was related to the suppression of CD44 expression, thus *p53* mutation could contribute to enhancing the expression of CD44 in Ov-associated CCA.<sup>(48)</sup>

Taken together, our present results lead to the conclusion that an accumulation of CD44v8–10 causes suppression of p38<sup>MAPK</sup> expression in transforming bile duct cells and links to a poor prognosis in CCA patients. Depletion of CD44v8–10 induced the loss of xCT from the cell surface and increased the ROS level in an *in vitro* model. Sulfasalazine could suppress cell growth and trigger autophagic cell death. Therefore, an xCT-targeting drug may improve CCA treatment by sensitizing CCA cells to the available chemotherapeutic drugs (e.g., gemcitabine) by blocking the mechanism of the cell's ROS defensive system.

## Acknowledgments

This research was supported by the Thailand Research Fund through the Royal Golden Jubilee Ph.D. Program (Grant No. PHD/0191/2552) and Khon Kaen University Research Fund; a grant from the Faculty of Medicine, Khon Kaen University (Grant No. I56327); a grant from the Higher Education Research Promotion and National Research University Project of Thai-land, Office of the Higher Education Commission, through the Health Cluster (SHeP-GMS); and a grant from the Ministry of Education, Culture, Sports, Science and Technology of Japan (HS#22130007 and S1411037). We thank Professor Trevor Petney for English assistance.

**Disclosure Statement**

The authors have no conflict of interest.

**Abbreviations**

Atg	autophagy-related
BSO	buthionine sulphoximine
CCA	cholangiocarcinoma
CD44s	standard CD44
CD44v	CD44 variant

CSC	cancer stem cell
DCF	dichlorofluorescein
DCFH-DA	dichloro-dihydro-fluorescein diacetate
GSH	reduced glutathione
IHC	immunohistochemical
LC3	microtubule-associated protein 1A/1B-light chain 3
Ov	<i>Opisthorchis viverrini</i>
ROS	reactive oxygen species
SSZ	sulfasalazine
Trolox	6-hydroxy-2,5,7,8-tetramethylchroman-2-carboxylic acid

**References**

- Zoller M. CD44: can a cancer-initiating cell profit from an abundantly expressed molecule? *Nat Rev Cancer* 2011; **11**: 254–67.
- Nagano O, Okazaki S, Saya H. Redox regulation in stem-like cancer cells by CD44 variant isoforms. *Oncogene* 2013; **32**: 5191–8.
- Al-Hajj M, Wicha MS, Benito-Hernandez A, Morrison SJ, Clarke MF. Prospective identification of tumorigenic breast cancer cells. *Proc Natl Acad Sci USA* 2003; **100**: 3983–8.
- Collins AT, Berry PA, Hyde C, Stower MJ, Maitland NJ. Prospective identification of tumorigenic prostate cancer stem cells. *Cancer Res* 2005; **65**: 10946–51.
- Dalerba P, Dylla SJ, Park IK *et al*. Phenotypic characterization of human colorectal cancer stem cells. *Proc Natl Acad Sci USA* 2007; **104**: 10158–63.
- Prince ME, Sivanandan R, Kaczorowski A *et al*. Identification of a subpopulation of cells with cancer stem cell properties in head and neck squamous cell carcinoma. *Proc Natl Acad Sci USA* 2007; **104**: 973–8.
- Bannai S, Ishii T. Transport of cystine and cysteine and cell growth in cultured human diploid fibroblasts: effect of glutamate and homocysteate. *J Cell Physiol* 1982; **112**: 265–72.
- Kim GY, Mercer SE, Ewton DZ, Yan Z, Jin K, Friedman E. The stress-activated protein kinases p38 alpha and JNK1 stabilize p21(Cip1) by phosphorylation. *J Biol Chem* 2002; **277**: 29792–802.
- Hemmati PG, Normand G, Verdoordt B *et al*. Loss of p21 disrupts p14 ARF-induced G1 cell cycle arrest but augments p14 ARF-induced apoptosis in human carcinoma cells. *Oncogene* 2005; **24**: 4114–28.
- Muller M. Cellular senescence: molecular mechanisms, *in vivo* significance, and redox considerations. *Antioxid Redox Signal* 2009; **11**: 59–98.
- Baldi A, Piccolo MT, Boccellino MR *et al*. Apoptosis induced by piroxicam plus cisplatin combined treatment is triggered by p21 in mesothelioma. *PLoS ONE* 2011; **6**: e23569.
- Liao PC, Ng LT, Lin LT, Richardson CD, Wang GH, Lin CC. Resveratrol arrests cell cycle and induces apoptosis in human hepatocellular carcinoma Huh-7 cells. *J Med Food* 2010; **13**: 1415–23.
- Sripa B, Kaewkes S, Sithithaworn P *et al*. Liver fluke induces cholangiocarcinoma. *PLoS Med* 2007; **4**: e201.
- IARC. Infection with liver flukes (*Opisthorchis viverrini*, *Opisthorchis felinus* and *Clonorchis sinensis*). *IARC Monogr Eval Carcinog Risks Hum* 1994; **61**: 121–75.
- Sithithaworn P, Yongvanit P, Duengngai K, Kiatsopit N, Pairojkul C. Roles of liver fluke infection as risk factor for cholangiocarcinoma. *J Hepatobiliary Pancreat Sci* 2014; **21**: 301–8.
- Yongvanit P, Pinlaor S, Loilome W. Risk biomarkers for assessment and chemoprevention of liver fluke-associated cholangiocarcinoma. *J Hepatobiliary Pancreat Sci* 2014; **21**: 309–15.
- Thanan R, Oikawa S, Hiraku Y *et al*. Oxidative stress and its significant roles in neurodegenerative diseases and cancer. *Int J Mol Sci* 2015; **16**: 193–217.
- Thanan R, Techasen A, Hou B *et al*. Development and characterization of a hydrogen peroxide-resistant cholangiocyte cell line: A novel model of oxidative stress-related cholangiocarcinoma genesis. *Biochem Biophys Res Commun* 2015; **464**: 182–8.
- Jusakul A, Loilome W, Namwat N *et al*. Anti-apoptotic phenotypes of cholestan-3beta,5alpha,6beta-triol-resistant human cholangiocytes: characteristics contributing to the genesis of cholangiocarcinoma. *J Steroid Biochem Mol Biol* 2013; **138**: 368–75.
- Sugihara E, Saya H. Complexity of cancer stem cells. *Int J Cancer* 2013; **132**: 1249–59.
- Huang Y, Dai Z, Barbacioru C, Sadee W. Cystine-glutamate transporter SLC7A11 in cancer chemosensitivity and chemoresistance. *Cancer Res* 2005; **65**: 7446–54.
- Ishimoto T, Nagano O, Yae T *et al*. CD44 variant regulates redox status in cancer cells by stabilizing the xCT subunit of system xc(–) and thereby promotes tumor growth. *Cancer Cell* 2011; **19**: 387–400.
- Lo M, Ling V, Wang YZ, Gout PW. The xc<sup>–</sup> cystine/glutamate antiporter: a mediator of pancreatic cancer growth with a role in drug resistance. *Br J Cancer* 2008; **99**: 464–72.
- Guan J, Lo M, Dockery P *et al*. The xc<sup>–</sup> cystine/glutamate antiporter as a potential therapeutic target for small-cell lung cancer: use of sulfasalazine. *Cancer Chemother Pharmacol* 2009; **64**: 463–72.
- Chen RS, Song YM, Zhou ZY *et al*. Disruption of xCT inhibits cancer cell metastasis via the caveolin-1/beta-catenin pathway. *Oncogene* 2009; **28**: 599–609.
- Zhang W, Trachootham D, Liu J *et al*. Stromal control of cystine metabolism promotes cancer cell survival in chronic lymphocytic leukaemia. *Nat Cell Biol* 2012; **14**: 276–86.
- Yoshikawa M, Tsuchihashi K, Ishimoto T *et al*. xCT inhibition depletes CD44v-expressing tumor cells that are resistant to EGFR-targeted therapy in head and neck squamous cell carcinoma. *Cancer Res* 2013; **73**: 1855–66.
- Thamavit W, Bhamarapavati N, Sahaphong S, Vajrasthira S, Angsubhakorn S. Effects of dimethylnitrosamine on induction of cholangiocarcinoma in *Opisthorchis viverrini*-infected Syrian golden hamsters. *Cancer Res* 1978; **38**: 4634–9.
- Loilome W, Yongvanit P, Wongkham C *et al*. Altered gene expression in *Opisthorchis viverrini*-associated cholangiocarcinoma in hamster model. *Mol Carcinog* 2006; **45**: 279–87.
- Dechakhamphu S, Pinlaor S, Sithithaworn P, Bartsch H, Yongvanit P. Accumulation of miscoding etheno-DNA adducts and highly expressed DNA repair during liver fluke-induced cholangiocarcinogenesis in hamsters. *Mutat Res* 2010; **691**: 9–16.
- Hsu SM, Raine L. Protein A, avidin, and biotin in immunohistochemistry. *J Histochem Cytochem* 1981; **29**: 1349–53.
- Jamnongkan W, Techasen A, Thanan R *et al*. Oxidized alpha-1 antitrypsin as a predictive risk marker of opisthorchiasis-associated cholangiocarcinoma. *Tumour Biol* 2013; **34**: 695–704.
- Yothaisong S, Dokduang H, Techasen A *et al*. Increased activation of PI3K/AKT signaling pathway is associated with cholangiocarcinoma metastasis and PI3K/mTOR inhibition presents a possible therapeutic strategy. *Tumour Biol* 2013; **34**: 3637–48.
- Thanee M, Loilome W, Techasen A *et al*. Quantitative changes in tumor-associated M2 macrophages characterize cholangiocarcinoma and their association with metastasis. *Asian Pac J Cancer Prev* 2015; **16**: 3043–50.
- Ito T, Sakurai-Yageta M, Goto A, Pairojkul C, Yongvanit P, Murakami Y. Genomic and transcriptional alterations of cholangiocarcinoma. *J Hepatobiliary Pancreat Sci* 2014; **21**: 380–7.
- Chen BL, Guo K, Liu YK. Relationship between CD44 expression or glycosylation and hepatocellular carcinoma metastasis. *Zhonghua Gan Zang Bing Za Zhi* 2011; **19**: 898–903.
- Ishimoto T, Oshima H, Oshima M *et al*. CD44+ slow-cycling tumor cell expansion is triggered by cooperative actions of Wnt and prostaglandin E2 in gastric tumorigenesis. *Cancer Sci* 2010; **101**: 673–8.
- Kunlabut K, Vaeteewoottacharn K, Wongkham C *et al*. Aberrant expression of CD44 in bile duct cancer correlates with poor prognosis. *Asian Pac J Cancer Prev* 2012; **13**(Suppl): 95–9.
- Pongcharoen P, Jinawath A, Tohtong R. Silencing of CD44 by siRNA suppressed invasion, migration and adhesion to matrix, but not secretion of MMPs, of cholangiocarcinoma cells. *Clin Exp Metastasis* 2011; **28**: 827–39.
- Cui Q, Tashiro S, Onodera S, Minami M, Ikejima T. Oridonin induced autophagy in human cervical carcinoma HeLa cells through Ras, JNK, and P38 regulation. *J Pharmacol Sci* 2007; **105**: 317–25.
- Kim DS, Kim JH, Lee GH *et al*. p38 Mitogen-activated protein kinase is involved in endoplasmic reticulum stress-induced cell death and autophagy in human gingival fibroblasts. *Biol Pharm Bull* 2010; **33**: 545–9.
- Lim SC, Hahm KS, Lee SH, Oh SH. Autophagy involvement in cadmium resistance through induction of multidrug resistance-associated protein and counterbalance of endoplasmic reticulum stress WI38 lung epithelial fibroblast cells. *Toxicology* 2010; **276**: 18–26.

- 43 Verrey F, Closs EI, Wagner CA, Palacin M, Endou H, Kanai Y. CATs and HATs: the SLC7 family of amino acid transporters. *Pflugers Arch* 2004; **447**: 532–42.
- 44 Gout PW, Buckley AR, Simms CR, Bruchovsky N. Sulfasalazine, a potent suppressor of lymphoma growth by inhibition of the x(c)- cystine transporter: a new action for an old drug. *Leukemia* 2001; **15**: 1633–40.
- 45 Dechakhamphu S, Yongvanit P, Nair J, Pinlaor S, Sitthithaworn P, Bartsch H. High excretion of etheno adducts in liver fluke-infected patients: protection by praziquantel against DNA damage. *Cancer Epidemiol Biomarkers Prev* 2008; **17**: 1658–64.
- 46 Pinlaor S, Yongvanit P, Hiraku Y *et al.* 8-nitroguanine formation in the liver of hamsters infected with *Opisthorchis viverrini*. *Biochem Biophys Res Commun* 2003; **309**: 567–71.
- 47 Chan-On W, Nairismagi ML, Ong CK *et al.* Exome sequencing identifies distinct mutational patterns in liver fluke-related and non-infection-related bile duct cancers. *Nat Genet* 2013; **45**: 1474–8.
- 48 Tamada M, Nagano O, Tateyama S *et al.* Modulation of glucose metabolism by CD44 contributes to antioxidant status and drug resistance in cancer cells. *Cancer Res* 2012; **72**: 1438–48.